Electron-vibron–breather interaction

Dirk Hennig
Freie Universität Berlin, Fachbereich Physik, Institut für Theoretische Physik, Arnimallee 14, 14195 Berlin, Germany
(Received 10 February 2000; revised manuscript received 14 April 2000)

We study the interaction of breathers in the context of a coupled electron-vibron lattice system. Starting with single-site excitations, it is demonstrated that constellations exist for which the coexistence of electronic and vibronic breathers is assured. The energy exchange between the vibrational and electronic subsystems and its impact on the breather formation are discussed in detail. The coupled electron-vibron dynamics shows a tendency toward energy redistribution into the vibronic degrees of freedom at the expense of the electronic energy content. Attention is paid to the relaxation dynamics in the energy exchange and we discuss the attainment of a steady regime for the coupled electron-vibron dynamics starting from a nonequilibrium state. It is demonstrated that the presence of breathers has a strong impact on the relaxation dynamics. Breathers can assist the relaxation process. With the help of a linear stability analysis, we show why the electronic subsystem acts as an energy donor while the vibron system serves as the energy acceptor. To this end we investigate the existence and stability of localized breathing eigenmodes capable of energy trapping. A frequency analysis reveals that strong exchange also occurs due to a temporal transition from single-frequency breathers to those oscillating with two frequencies and their temporal resonance interaction. Finally, the self-stabilized electron-vibron system relaxes to a combined electron-vibron breather. On increasing the electron-vibron coupling strength, only a vibronic phonobreather of large amplitude survives, whereas the electronic subsystem tends to energy equipartition.

PACS number(s): 41.20.Jb, 63.20.Pw, 63.20.Ry

I. INTRODUCTION

Discrete breathers, that is, spatially localized and time-oscillating solutions, of discrete nonlinear lattice systems have attracted considerable interest over recent years [1–23] (for reviews see [24,25]). Recently, rigorous results have been obtained concerning the existence and stability of breathers in nonlinear lattices [18,26,27]. Such intrinsic localized modes have been observed experimentally in electric networks [28], in Josephson ladders [29], in waveguide arrays [30], in a quasi-one-dimensional charge density wave system [31], and in crystalline arrays of charged linear chains of PtCl [31]. Breathers have been proposed to understand the transient photodynamics of various low-dimensional electronic materials such as conjugated polymers [32], and femtosecond chemistry allows one to probe the photophysics of breatherlike excitations [33]. The proper excitation of intrinsic localized modes of anharmonic lattices via optical control was discussed in [34].

A great deal of the theoretical research has been focused on the dynamical properties of breathers, such as their stability and mobility [6,8,23,35,36] and numerical algorithms for the excitation of breather solutions have been developed [37]. Furthermore, the impact of the internal structure of discrete breathers on their formation and stability properties has been investigated [12,13,38,39]. It has been demonstrated that perturbations along internal breathing modes of the discrete breathers can also cause breather bifurcations, e.g., from single-frequency breathers to those oscillating with more than one frequency. Moreover, when certain internal modes are properly excited the breather may become mobile [23,35]. Internal localized modes of breathers are also connected with scattering properties [40,41].

However, most breather studies have concerned homogeneous nonlinear lattice systems having one degree of freedom per lattice site (unit cell). These nonlinear lattices consist of coupled oscillators of one specific type, and the nonlinearity stems from the local anharmonicity of the on-site oscillators [Klein-Gordon (KG) chains] and/or is contained in the coupling terms [Fermi-Pasta-Ulam (FPU) models] [25]. Studies on several degrees of freedom per unit cell have been performed in [42–44]. From the perspective of localization, combinations of distinct lattices have been addressed in [45–56].

The present study is devoted to a combined lattice system possessing two different dynamical degrees of freedom per site. It describes the movement of an electron along a one-dimensional molecular chain modeled by a discrete nonlinear Schrödinger equation (DNLS) [57–65]. Moreover, the molecular constituents of the chain perform longitudinal vibrations described by a KG Hamiltonian. The electronic dispersion, viz., the transfer matrix element, depends on the relative elongation of two adjacent lattice sites and in this manner the coupling between the electronic and vibronic subsystems is established. Our model has to be distinguished from the Holstein model [45], its generalizations [52,53] and Davydov-type systems [46–55]. Basic to all these systems is the coupling between electronic (excitonic) and vibronic degrees of freedom in a combined lattice system.

The work in [54] considered the interaction of a single electron with a discrete breather in a nonlinear FPU lattice. The electron-lattice coupling arises through dependence of the electronic overlap integral in a one-dimensional electronic tight-binding description on the positions of the lattice sites. It is demonstrated that a bound electron-breather state exists. The electron localization arises as the result of its capture by the vibrational breather during each half period of its oscillation without any response of the electron to the

breather. The study in [55] dealt with the self-consistent interaction of a single electron with longitudinal FPU lattice vibrations when the electron response to the lattice breather is taken into account. Due to the presence of the electron in the lattice, a static lattice deformation creates a potential well for the electron as well as the lattice vibrations causing localization in the form of a coupled breatherlike state.

In [50,51] the electronic motion is studied in a single one-dimensional tight-binding band interacting with the vibrations of a nonlinear lattice. Attention is focused on the analysis of energy equilibration and electron motion starting in a highly nonequilibrium initial state. The nonlinear lattice considered in [50,51] does not itself support discrete breathers. An explanation for the absence of (pure) lattice vibration breathers is given by the fact that the existence criterion depending on the potential parameters of [66] is not fulfilled for the specific anharmonic lattice potential of [50,51] (see [54]). Nevertheless, a bound electron-vibron-breather state can exist due to the local alterations of the lattice energy (deformation of the lattice) caused by the initially localized electron creating a potential well not only for itself but also for the lattice vibrations. These combined bound states arise experimentally when incident electrons collide with a thin film [67]. On its way through the film the electron exchanges energy with the excitations of the material [68–70]. These processes also play an important role in nanoelectronics, such as quantum wells and wires [71–73]. Furthermore, initially highly nonequilibrium situations also occur experimentally when a localized electron (exciton) is produced by initial excitations, e.g., due to phototransfer. Again, this electron can distribute its energy during its motion in the material [74–76]. The advances in femtosecond spectroscopy make it possible to go to time and space scales for which the experimental study of transient phenomena of interacting electronic and vibrational subsystems is possible.

The studies in [50,51] considered the process of energy redistribution between an initially localized electron and the vibrations of an anharmonic lattice. The lattice atoms were assumed to be in their rest positions, having zero velocities. However, in contrast to the previous studies, in the current approach the electronic as well as vibronic lattice degrees of freedom are represented by a *nonlinear* lattice system, each system bearing its own breather solutions localizing electronic and vibrational energy, respectively. The coupling between the electronic and vibronic nonlinear systems then allows us to study the highly nonlinear interaction of electron and vibron breathers with respect to the time evolution of the energy redistribution in the combined lattice system. We think that the results are of relevance for the relaxation dynamics in real systems starting from a nonequilibrium excitation state and when nonlinear excitations are present in the interacting electronic as well as vibrational degrees of freedom.

The paper is organized as follows. In Sec. II we introduce the coupled electron-vibron lattice system and examine its coupled dynamics. With this aim a breather solution is launched in both subsystems and their combined development is observed with emphasis on the dynamics of the energy exchange between the electronic degrees of freedom and the vibronic ones. In detail, we discuss how the relaxation process in the energy redistribution is influenced by breather solutions. In Sec. III A we investigate the linear stability of the coupled breather dynamics. The time evolution of the eigenvalues of the Jacobian matrix corresponding to the system of linear equations in the tangent space is monitored. In particular, we study the existence and stability of internal localized modes and their impact on electronic and vibronic breather formation and stability, respectively. Based on a Fourier analysis we demonstrate that, during an interlude of strong electron-vibron interaction, a transition from single-frequency breathers to two-frequency breathers takes place. Finally, in Sec. IV we give a summary.

II. COUPLED ELECTRON-VIBRON SYSTEM

We consider the transfer of an electron along a one-dimensional molecular chain where the electron movement is influenced by longitudinal vibrations of the molecular constituents of the chain. The Hamiltonian is determined by

$$H = H_e + H_v , \tag{1}$$

with the electronic part given by a DNLS system derived from the Hamiltonian

$$H_e = E \sum_{n=1}^{N} |c_n|^2 + \frac{\gamma}{2} \sum_{n=1}^{N} |c_n|^4 + \sum_{n=1}^{N} V_{n\,n-1}(c_n^* c_{n-1} + c_n c_{n-1}^*), \tag{2}$$

where c_n represents the probability amplitude of the electron occupying the molecular site n and E is the on-site energy. The parameter γ regulates the strength of the nonlinearity that arises from the adiabatic elimination of local fast intramolecular vibrations strongly coupled to the electron amplitudes [46,57–65,77]. The derivation of this nonlinear electron (polaron) model is based on a time-scale separation argument, and in particular on the fact that the intramolecular vibrations are much faster than any intermolecular process (intermolecular electron transfer or the relative vibrational motion of the lattice sites). The third sum in Eq. (2) represents the kinetic electronic lattice energy where $V_{n\,n-1}$ is the transfer matrix element of the electronic coupling between two molecular lattice sites. The transfer matrix element depends on the intersite relative coordinate $q_n - q_{n-1}$ in a linear fashion,

$$V_{n\,n-1} = V_0[1 - a(q_n - q_{n-1})], \tag{3}$$

with q_n being the elongation of the nth molecular unit and a the coupling parameter. In the limit $a = 0$ the transfer element reduces to $V_0 = \text{const}$, and the Hamiltonian (2) yields the standard DNLS system.

The nonlinear classical dynamics of the longitudinal vibrations of the molecular sites is described by a Klein-Gordon lattice system with Hamiltonian

$$H_v=\frac{1}{2}\sum_{n=1}^{N}p_n^2+\frac{\omega_0^2}{2}\sum_{n=1}^{N}q_n^2+\frac{b}{4}\sum_{n=1}^{N}q_n^4 + \frac{1}{2}c\sum_{n=1}^{N}(q_n-q_{n-1})^2, \tag{4}$$

where ω_0 is the frequency of small amplitude oscillations of the lattice sites, bq_n^4 is the anharmonic part of the quartic on-site potential, and c is the coupling constant. It is through Eq. (3) that the coupling between the electronic and intersite vibrational degrees of freedom is introduced. Since the latter are not constant, the transfer matrix elements are modulated by the motion of the molecular sites relative to each other. When two adjacent units are further apart, the corresponding matrix element diminishes, causing a reduction in the electron transfer from one site to the other. Correspondingly, for two neighboring sites coming closer to each other the transfer matrix element increases, resulting in enhanced electron transfer. (For a quantum treatment of the lattice vibrations this would be a study of phonon-assisted hopping [78].) We do not take into account diagonal couplings of the vibrational and electronic degrees of freedom, since their effect on the electron-vibron dynamics is assumed to be dominated by the diagonal nonlinear polaronic γ term. Moreover, due to a simple phase transformation $\tilde{c}_n(t)=c_n(t)\exp(-iEt)$, the E dependence can be removed from the equations of motion.

III. COUPLED ELECTRON-VIBRON DYNAMICS, ENERGY REDISTRIBUTION, AND RELAXATION DYNAMICS

In this section we study the dynamics of the coupled electron-vibron motion in the context of the system given by Eqs. (1)–(4). The corresponding equations of motion are

$$i\dot{c}_n=\frac{\partial H}{\partial c_n^*}=\gamma|c_n|^2c_n+V_0[1-a(q_{n+1}-q_n)]c_{n+1} + V_0[1-a(q_n-q_{n-1})]c_{n-1}, \tag{5}$$

$$\dot{p}_n=-\frac{\partial H}{\partial q_n}=-\omega_0^2q_n-bq_n^3+c(q_{n+1}+q_{n-1}-2q_n) + aV_0(c_n^*c_{n-1}+c_nc_{n-1}^*)-aV_0(c_{n+1}^*c_n+c_nc_{n+1}^*), \tag{6}$$

$$\dot{q}_n=\frac{\partial H}{\partial p_n}=p_n. \tag{7}$$

In the limit of $a=0$ we obtain the pure DNLS lattice and a KG chain, each supporting breather solutions, corresponding to electron and vibron localization, respectively. In Fig. 1 we depict such breather solutions. We excited initially a single site electronically as well as vibrationally and all other sites were left in their rest positions. Such a local excitation of the coupled electron-vibron lattice can be viewed as the local injection of excitation energy by an external process (e.g., a laser pulse leaving a hot spot). During this process both the electronic degrees of freedom and the vibronic part become locally excited. The initial amplitudes are chosen

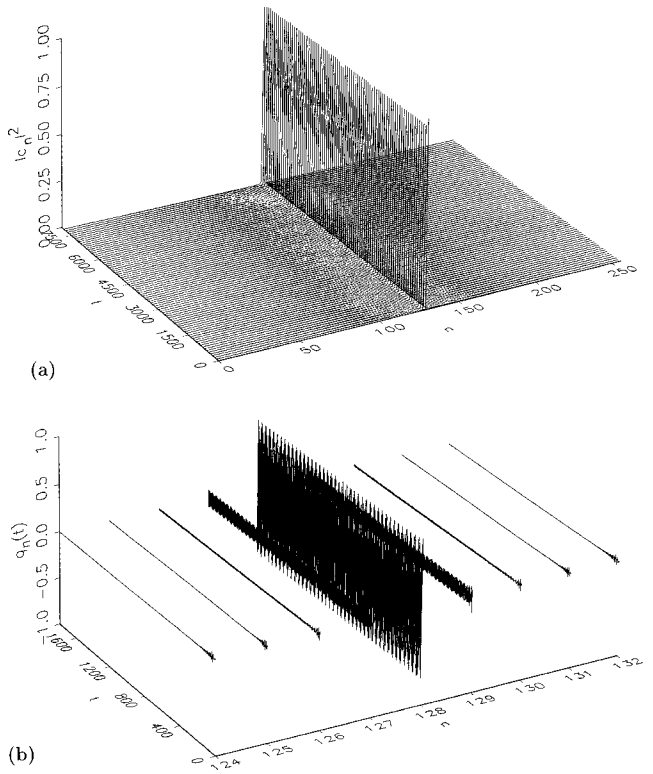

FIG. 1. The amplitude profile of the DNLS and KG lattices for vanishing electron-vibron coupling $a=0$. The lattice length is $N=256$ and periodic boundary conditions are imposed. (a) The DNLS lattice with initially excited central site, i.e., $x(0)_{128}=y(0)_{128}=1/\sqrt{2}$ and $x(0)_{n\neq128}=y(0)_{n\neq128}=0$. Shown is the electronic occupation amplitude $|c_n(t)|^2=x_n^2(t)+y_n^2(t)$. Parameters: $\gamma=1$ and $V_0=0.1$. (b) The KG lattice with initially excited central site, i.e., $q(0)_{128}=0.746$, $q(0)_{n\neq128}=0$, and $p(0)_{1\leq n\leq256}=0$. Shown is the vibronic coordinate $q_n(t)$. Parameters: $\omega_0=1/4$, $b=1$, and $c=0.05$.

such that the energy content of the two lattice chains does not differ significantly. According to [26] we expect that these single-site initial conditions will be continued as breather solutions if the coupling between the lattice oscillators is sufficiently small. (The mathematical proof of the existence of such a combined breather state will be presented elsewhere [79]). In fact, after an initial transient phase, both lattice dynamics have completely adopted stable breather solutions with exponentially decaying tails around the initially excited site. Each of their strongly localized excitation patterns involves mainly three sites. For the electronic breather, it is equivalent to a stationary solitonlike solution schematically expressed as

$$(\ldots\uparrow\begin{array}{|c}\uparrow\\ \\ \end{array}\ldots),$$

where the dots stand for vanishingly small amplitudes. This mode sustaining symmetry breaking perturbations of its pattern is centered at a single site [17,77]. On the KG lattice a similar spatially symmetric breather is formed. The formation process and the stability of the breathers are linked to the excitation of their internal localized modes as those eigenvectors of the system linearized around the breather which are localized too (see below in Sec. III A). Without the polaronic term, i.e., with $\gamma=0$ in Eq. (5), the electronic

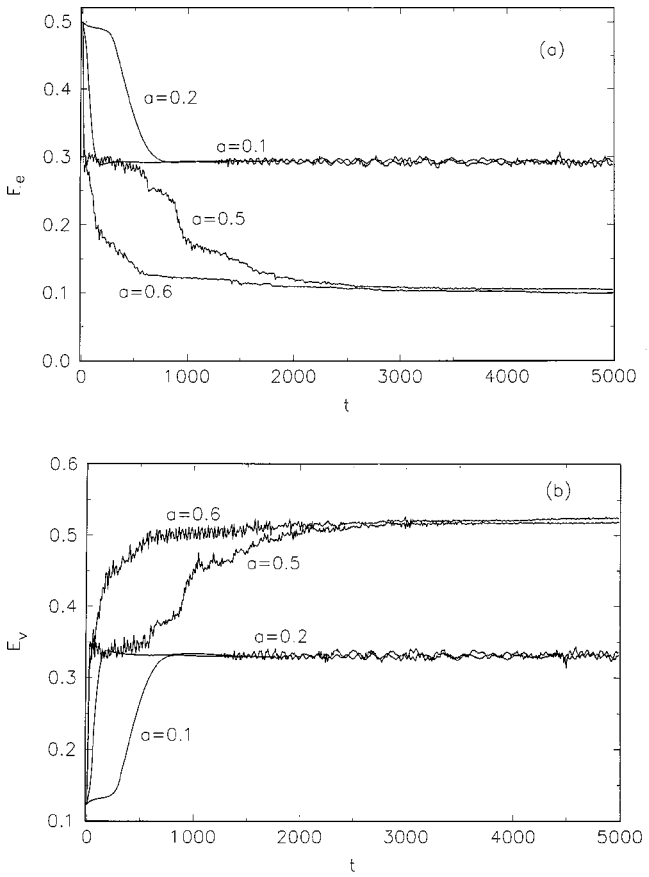

FIG. 2. Temporal evolution of the partial energies for the coupled DNLS and KG lattices for different electron-vibron coupling strengths a as indicated. Initial conditions and parameters as in Fig. 1. $E_e(E_v)$ indicates the electronic (vibronic) energy. (a) The electronic energy E_e. (b) The vibronic energy E_v.

probability amplitude would spread all over the lattice in the course of time, leading to a delocalized electron.

The aim of the current paper is to investigate the breather interaction in the context of a coupled nonlinear electron-vibron model with particular respect to the transient dynamics of the electron-vibron energy redistribution. In Fig. 2 we depict the temporal evolution of the partial energies of the electronic and vibronic subsystems for different strengths of the interaction a. [The contribution of the interaction energy $H_{int}=a\Sigma_n(q_n-q_{n-1})(c_n^*c_{n-1}+c_nc_{n-1}^*)$ to the total energy is less than 1%.] We always observe redistribution of the electronic energy into the vibronic subsystem, regardless of the coupling strength. The coupling of the localized electron to its surrounding lattice sites causes local lattice displacements. As a consequence, lattice modes differing in their phases and velocities become excited and their superpositions may extend with time over the KG lattice. This spreading behavior is manifested also in a temporal increase of the lattice partition number, measuring the distribution of the excitation energy among the lattice sites (see Fig. 6 below). Since the number of excited vibrational lattice modes is fairly high it seems unlikely that energy flows back into the electronic degrees of freedom. Thus the process of energy redistribution from the electronic degrees of freedom into the vibronic ones is irreversible (see also [51]).

For weak coupling ($a\lesssim 0.25$) the energy exchange is not too strong. After an initial transient phase of gradual electronic (vibronic) energy loss (gain), no further vibrational band states get excited, so that the energy redistribution process terminates and the curves reach plateaus of constant, nearly balanced, partial energies corresponding to a steady equilibrium state. This striking feature shows us that after a local deposition of excitation energy a transient of directed energy transfer from the electronic to the vibronic subsystem takes place until an equilibrium situation is attained. Note the small amplitude oscillations around the steady state energy values. The physical meaning is that a small part of the vibrational energy is fed back into the electronic state and this amount of energy is from then on transferred between the electronic and vibronic subsystems. On both the KG and the DNLS lattices a stable breather has been created. The formation process of an electronic (vibronic) breather is very similar to that in the uncoupled case shown in Fig. 1. Regarding the electron breather, we notice an initial phase during which the breather amplitude diminishes while its localized shape is conserved. Eventually, after approximately 1000 time units the amplitude loss terminates and a stable (stationary) electron breather remains with this reduced but virtually constant amplitude. Accordingly, the vibronic part accumulates the energy released by the electronic subsystem. Let us recall that the initial single-site excitation of the vibrational lattice causes a trapping potential for the nonlinear lattice vibrations themselves. As a matter of fact, the spatiotemporal amplitude pattern of the KG lattice relaxes onto its own breather solutions for a single-site initial excitation [see Fig. 1(b)], maintaining localization at the initial site, so that finally the dispersion of the vibrational excitation energy is inhibited. In addition, the lattice vibrations are influenced by a trapping potential created by their coupling to the localized electron. During the short time transient process of gradual decrease of electronic energy, the electron itself remains localized at its initially excited site and experiences only a steady reduction of its amplitude in accordance with the loss of its energy.

In general, the larger the coupling a the less time it takes to reach the equilibrium state, and the amount of electronic energy distributed into the vibrational lattice also gets larger. Moreover, for $a\gtrsim 0.5$ there is at the beginning a sudden increase (decrease) of the vibrational (electronic) energy as if the lattice oscillators experience an instant kicklike distortion by the localized electron. Unlike the exchange dynamics in the low-coupling case ($a\lesssim 0.2$), here there already appear small amplitude oscillations during the transient redistribution phase, pointing to early time energy backfeeding of tiny portions of vibronic energy into the electronic system, and vice versa. We further observe that after short times each curve still reaches a plateau; however, the amplitudes of the oscillations around the corresponding steady energy value decay more rapidly the larger the coupling. With regard to the amplitude patterns of the lattices, we note that for $2\lesssim a \lesssim 0.6$ a stable electronic breather on the DNLS lattice has been formed, whereas on the KG lattice we observe a breather solution at the initially excited site which is surrounded by small amplitude phononic excitations. Apparently, the stronger the electron-vibron coupling the greater is the impact of the localized electron on the lattice vibrations. The large amount of electronic energy injected rapidly and

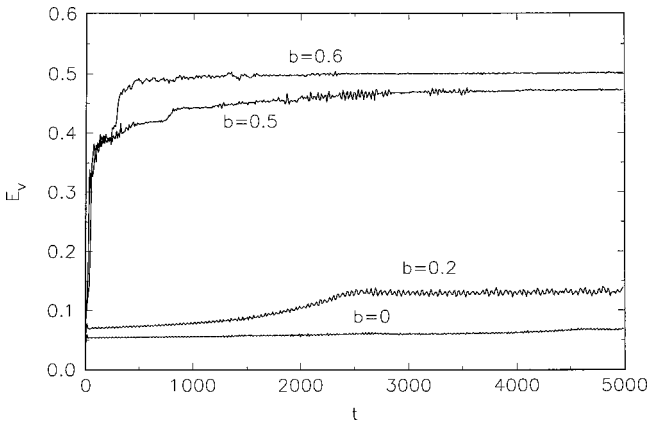

FIG. 3. Temporal evolution of the vibrational lattice energy E_{vib} for different nonlinearity strengths b and fixed electron-vibron coupling strength $a=0.5$.

locally into the KG lattice can exceed the trapping ability of the initial nonlinear KG lattice site, and thus the excess energy that cannot be pinned there has to be rejected such that phononic modes are excited, which disperse into extended parts of the KG lattice. Afterwards, when the partial energies evolve around the equilibrium plateaus, we observe an in-phase motion of the electronic potential (kinetic) and the vibronic kinetic (potential) energies, whereas the potential and kinetic energies of each lattice oscillate out of phase. In other words, the impact of the localized electron on the central lattice oscillator results in a temporal increase of the vibronic potential energy due to larger elongations of the lattice oscillator, which in turn leads to an enlarged local electronic transfer matrix element (electronic kinetic energy). The increase in the electronic kinetic energy goes along with an attempt to delocalize the electron and thus weakens the local influence of the electron-vibron interaction around the initially excited site. On the other hand, the strongly localized electron does not leave the near vicinity of the initial site, and only a small portion of the electronic excitation energy oscillates between the central site and its left and right adjacent sites, in accordance with the periodic change of the electronic kinetic and potential energy. At the moment when the latter reaches its maximum value, that is, when for vanishing electronic kinetic energy the electron is completely localized at the initially excited site, there is again a maximal influence of the electronic occupation on the vibrational central amplitude, and the energy exchange dynamics passes through another cycle. The resulting small amplitude oscillations in the temporal evolution of the partial energies decay more rapidly the larger the electron vibron coupling.

The threshold behavior, i.e., the sudden quantitative change in the energy exchange dynamics around some critical value of the coupling strength, is a genuine nonlinear effect. To gain further insight we illustrate in Fig. 3 the temporal development of the vibrational energy for a coupling strength $a=0.5$ and different nonlinearity strengths b of the KG lattice. (Because of energy conservation we can readily infer the corresponding evolution of the electronic energy from these pictures.) For comparison with the results in Fig. 2 we remark that the electron-vibron coupling $a=0.5$ is taken to be relatively large. Heavy directed energy migration occurs from the electronic to the vibronic subsystem for strong nonlinearity $b=1$, as seen in Fig. 2(b). For small b there is almost no variation of the vibronic (electronic) energy in the course of time. However, for $b\gtrsim 0.5$ this behavior changes drastically. At short times the vibronic energy jumps up to a higher value (analogous to the instant kicking behavior appearing in Fig. 2 for $a\geqslant 0.5$), increasing gradually afterward, and eventually reaches a horizontal plateau. While the DNLS lattice dynamics is characterized by stable electronic breathers regardless of the value of b, the localization properties of the vibronic KG lattice dynamics depend heavily on the value of the nonlinearity parameter. For the cases ($b=0$) and ($b=0.2$) in Fig. 3 there exists no strong vibron localization and we observe rather a small amplitude breathing localized state at the initially excited KG lattice site, from which small amplitude bandlike vibrations leak out into the remaining sites of the KG lattice. Apparently, it needs a certain overcritical nonlinearity strength b of the quartic potential in order to suppress dispersion. Starting from the case of $b=0$, i.e., a harmonic vibron lattice, it becomes clear that bound state creation requests at least a balance between two competing mechanisms: the tendency to disperse the vibronic energy (which is most efficient for the harmonic potential of $b=0$) due to the coupling among the vibron lattice oscillators, and, on the other hand, the trapping of the vibrational state itself by intrinsic KG nonlinearity (amplified with growing stiffness b of the potential), and additionally vibron trapping because of its coupling to the localized electronic amplitude. Conversely, only in the presence of a stable KG breather does the coupling between the electron and the vibron maintain a strong local character and the lattice vibrations absorb electronic energy efficiently. Otherwise, on dispersing vibronic energy away from the initially excited site, the electronic amplitude becomes nearly unaffected by the depleting vibrational amplitude. This is similar to the localization behavior in the opposite case, when the vibrational subsystem bears the nonlinearity whereas the electronic subsystem is described by a linear tight-binding lattice [50,51]. Strong enough electron-vibron interaction, determining the nonlinearity strength in this model, causes local deformations of the vibrational lattice, which create a potential well for the electronic amplitude and thus produce a polaronic state of the coupled electron-vibron lattice. Equivalently, in the present case the strong coupling of the localized electron to a weakly nonlinear KG lattice (small b) is able to generate a trapping potential for the single-site vibrational excitation, leading to a long time localization of the vibrational energy at the initially excited site. With enhanced nonlinearity strength b, not only is pronounced directed energy migration from the electronic to the vibronic subsystem initiated as reported above (see Fig. 2), but also the degree of vibron localization is amplified. Moreover, the larger b the higher is the amount of electronic energy absorbed by the vibron lattice and the less time it takes to achieve the equilibrium regime. This result demonstrates the accelerating effect of higher-amplitude vibron breathers on the relaxation process in highly excited systems.

From the perspective of the influence of the electronic breather on the relaxation dynamics, similar results are obtained when we vary the polaronic nonlinearity strength γ and keep all the other parameters fixed. For small $\gamma\lesssim 0.5$ the energy exchange behavior is equivalent to the cases of small

vibrational nonlinearity strength b illustrated in Fig. 2(b). Beyond a critical value ($\gamma \simeq 0.9$) the energy gain of the vibronic subsystem is again high and resembles the behavior of the strong coupling cases $a \geqslant 0.5$ in Fig. 2. However, when $\gamma \gtrsim 1.2$ there is no longer an energy redistribution from the electronic system into the vibronic degrees of freedom and the electronic and vibronic energy are conserved. The large polaronic term is then responsible for such a strong localization of the electronic energy at the initial site that the interaction between the two subsystems is actually suppressed. This prevention of the directed energy transfer from the electronic into the vibronic subsystem might have consequences for the vibron localization if b is not too large. In this case, the KG lattice may lack the amount of absorbed electronic energy needed to enhance its effective nonlinearity, that is, the amplitude of the initially excited site, which allows for profound vibron localization as in the cases previously discussed. Nevertheless, we observe a breathing localized vibron state at the initially excited lattice site, although it coexists with a background of small amplitude modes in the remainder of the KG lattice.

A. Linear stability and local internal modes

To gain deeper insight into the process of directed energy transfer from the electronic state into the vibronic one and to support the physical explanations given above by dynamical system arguments, we study the linear stability of the coupled breather dynamics. The two subsystems' responses to the mutual perturbations caused by their coupling may lead to the excitation of localized internal modes. The latter play a fundamental role in the formation and stability of breathers [25,38,39]. Thus we are especially interested in the existence and stability of localized internal modes. Imposing small perturbations

$$p_n(t) = p_n^{(0)}(t) + u_n(t), \quad q_n(t) = q_n^{(0)}(t) + v_n(t), \tag{8}$$

$$x_n(t) = x_n^{(0)}(t) + \xi_n(t), \quad y_n(t) = y_n^{(0)} + \eta_n(t), \tag{9}$$

substituting Eqs. (8) and (9) into the system (5)–(7), and linearizing around ($u_n = v_n = \xi_n = \eta_n = 0$) gives the linear system of tangent equations

$$\begin{aligned}\dot{u}_n = {} & c v_{n-1} - [\omega_0^2 + 3(q_n^{(0)})^2 + 2c] v_n + c v_{n+1} \\ & + 2aV_0[x_n^{(0)}\xi_{n-1} + (x_{n-1}^{(0)} - x_{n+1}^{(0)})\xi_n - x_n^{(0)}\xi_{n+1}] \\ & + 2aV_0[y_n^{(0)}\eta_{n-1} + (y_{n-1}^{(0)} - y_{n+1}^{(0)})\eta_n - y_n^{(0)}\eta_{n+1}],\end{aligned} \tag{10}$$

$$\dot{v}_n = u_n, \tag{11}$$

$$\begin{aligned}\dot{\xi}_n = {} & aV_0[y_{n-1}^{(0)} v_{n-1} + (y_{n+1}^{(0)} - y_{n-1}^{(0)}) v_n - y_{n+1}^{(0)} v_{n+1}] \\ & + 2\gamma x_n^{(0)} y_n^{(0)} \xi_n + V_0[1 - a(q_n^{(0)} - q_{n-1}^{(0)})]\eta_{n-1} \\ & + \gamma[(x_n^{(0)})^2 + 3(y_n^{(0)})^2]\eta_n \\ & + V_0[1 - a(q_{n+1}^{(0)} - q_n^{(0)})]\eta_{n+1},\end{aligned} \tag{12}$$

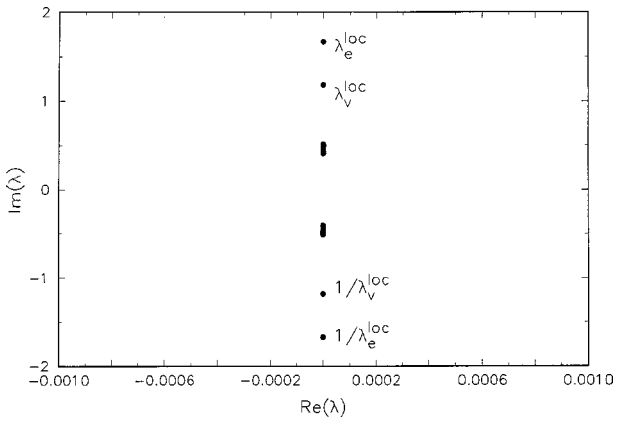

FIG. 4. Spectrum of the eigenvalues of the Jacobian matrix for the uncoupled DNLS KG lattice in the complex λ plane. Parameters and initial conditions as in Fig. 1. The two pairs of isolated eigenvalues corresponding to local breathing modes are denoted by $\lambda_e, 1/\lambda_e$ for the DNLS lattice and $\lambda_v, 1/\lambda_v$ for the KG lattice.

$$\begin{aligned}\dot{\eta}_n = {} & -aV_0[x_{n-1}^{(0)} v_{n-1} + (x_{n+1}^{(0)} - x_{n-1}^{(0)}) v_n - x_{n+1}^{(0)} v_{n+1}] \\ & - \gamma[3(x_n^{(0)})^2 + (y_n^{(0)})^2]\xi_n - V_0[1 - a(q_n^{(0)} - q_{n-1}^{(0)})]\xi_{n-1} \\ & - V_0[1 - a(q_{n+1}^{(0)} - q_n^{(0)})]\xi_{n+1} - 2\gamma x_n^{(0)} y_n^{(0)} \eta_n.\end{aligned} \tag{13}$$

Introducing the perturbation vector $\Delta = (u, v, \xi, \eta)$, we express the system (10)–(13) in matrix notation as

$$\dot{\Delta} = M\,\Delta, \tag{14}$$

where the Jacobian matrix $M = M(p(t), q(t), x(t), y(t))$ is determined via the right hand sides of the system (10)–(13). Linear stability of the solution $(p_n(t), q_n(t), x_n(t), y_n(t))$ requires that the Jacobian matrix M has no eigenvalue with positive real part, otherwise perturbations grow in time. The matrix M is symplectic. Therefore its complex eigenvalues occur in quadruples $(\lambda_k, \lambda_k^{-1}, \lambda_k^*, \lambda_k^{*-1})$ with $1 \leqslant k \leqslant N$.

During the transient process it is suitable to discuss the stability by inspection of the temporal development of the eigenvalues λ_n of the Jacobian matrix determining the temporal Lyapunov exponents. Before embarking on the coupled case, we briefly describe the features of the spectrum of the uncoupled case ($a = 0$) in the presence of individual stable electronic and vibronic breathers. The λ spectrum is shown in Fig. 4 in the complex plane. We recognize that the purely imaginary eigenvalues constitute two continuum bands corresponding to extended phonon modes. The frequency ranges of the linear bands are bounded by

$$-2V_0 \leqslant \omega_e \leqslant 2V_0, \tag{15}$$

$$\omega_0^2 \leqslant \omega_v^2 \leqslant \omega_0^2 + 4c, \tag{16}$$

where $\omega_e(\omega_v)$ denotes the phonon frequency of the DNLS (KG) chain. The eigenvalues with the largest (smallest) modulus of the imaginary part correspond to phonons with wave vector $0\ (\pi)$. For later reference we note that the upper edge of the KG phonon band is at the level $0.512i$. Furthermore, two pairs of isolated imaginary eigenvalues $(\lambda_e^{loc}, 1/\lambda_e^{loc})$ and $(\lambda_v^{loc}, 1/\lambda_v^{loc})$ are situated outside the bands of the phonon eigenvalues. The superscript *loc* indicates that

the corresponding eigenvectors of the Jacobian matrix represent localized breathing modes [25,38,39]. Due to the time reversibility of the breather solutions the corresponding pairs of eigenvectors (u_n^{loc}, v_n^{loc}) and $(\xi_n^{loc}, \eta_n^{loc})$ are complex conjugate, so that one is the image of the other through time reversibility. In particular, for the KG lattice it holds that $\mathrm{Im}\, v_n^{loc} = \mathrm{Re}\, u_n^{loc} = 0$, meaning that the momentum components are purely imaginary whereas the position components are real. For the DNLS lattice the stable eigenvectors satisfy either $\mathrm{Im}\, \eta_n^{loc} = \mathrm{Re}\, \xi_n^{loc} = 0$ or $\mathrm{Re}\, \eta_n^{loc} = \mathrm{Im}\, \xi_n^{loc} = 0$. Moreover, the internal local modes resemble the spatial symmetry of the (uncoupled) electronic and vibronic breathers.

For the coupled case of $a = 0.1$ we monitor the temporal evolution of the λ_n's and report time snapshots of their momentary positions in the complex plane. As an orientation for our description we use the spectrum of the uncoupled case shown in Fig. 4. Due to the reflection symmetry along the real axis it suffices to consider only the upper half of the complex λ plane, and in what follows we describe the temporal movement of the eigenvalues with positive imaginary part.

We distinguish three time intervals.

(i) $0 \leqslant t < 300$. The first snapshot is taken after a hundred time units. Most strikingly, the imaginary part of the vibronic isolated eigenvalue λ_v^{loc} has almost descended to the $k = 0$ edge of the phonon band. In general, we observe that eigenvalues may slightly depart from the imaginary axis into the right or left half plane but their real parts are confined to values in the interval $(-0.0001, 0.0001)$. Moreover, after a short duration, of the order of 50 time units, in one of the half planes the eigenvalues cross the imaginary axis, reversing the sign of their real part. These oscillatory crossings of the imaginary axis take place only for $t \lesssim 1000$. Therefore it is justified to discard the tiny real parts because they cause merely a negligible temporal amplitude change of the eigenfunctions. Afterward, for $t > 1000$, the eigenvalues come to lie on the imaginary axis. Since $\mathrm{Im}\, \lambda_v^{loc} = 0.517$ is just above the upper edge of the phonon band, its eigenfunction is only quasilocalized because the localization length is rather large [80]. In Fig. 5(a) we show the real part of the position component v_n^{loc} of the corresponding (normalized) eigenvector exhibiting a density group centered around the lattice site $n = 95$. We remark that the imaginary parts of the position components v_n^{loc} of the eigenvectors and the real parts of their momentum components u_n^{loc} are no longer zero but remain small. Most importantly, the asymmetric spatial patterns of the KG eigenvector shown in Fig. 5(a) break the spatial symmetry of the single-site excitation. Unlike the DNLS lattice, the KG lattice so far lacks the existence of a local breathing mode serving for strong localization of the initial conditions. Therefore the initial single-site vibronic excitation caused by a quasilocalized mode tends to disperse immediately into neighboring sites. This is why the vibronic lattice participation number $\overline{E_v}$ makes an early jump to relatively high values for $t > 0$ (see below). In contrast, perturbations of the DNLS breather by the stable localized eigenmode belonging to the isolated eigenvalue $\lambda_e^{loc} = 1.24i$ do not destroy the localization of the electronic energy at the initially excited site because the single-site breather and the perturbational mode have the the same spatial symmetry pattern strongly localized around the central lattice site. In Fig. 5(c) we draw the $\mathrm{Re}\, \xi_n^{loc}$ component of the strongly localized symmetric eigenmode of the DNLS chain to emphasize the difference from the quasilocalized eigenmode of the KG system.

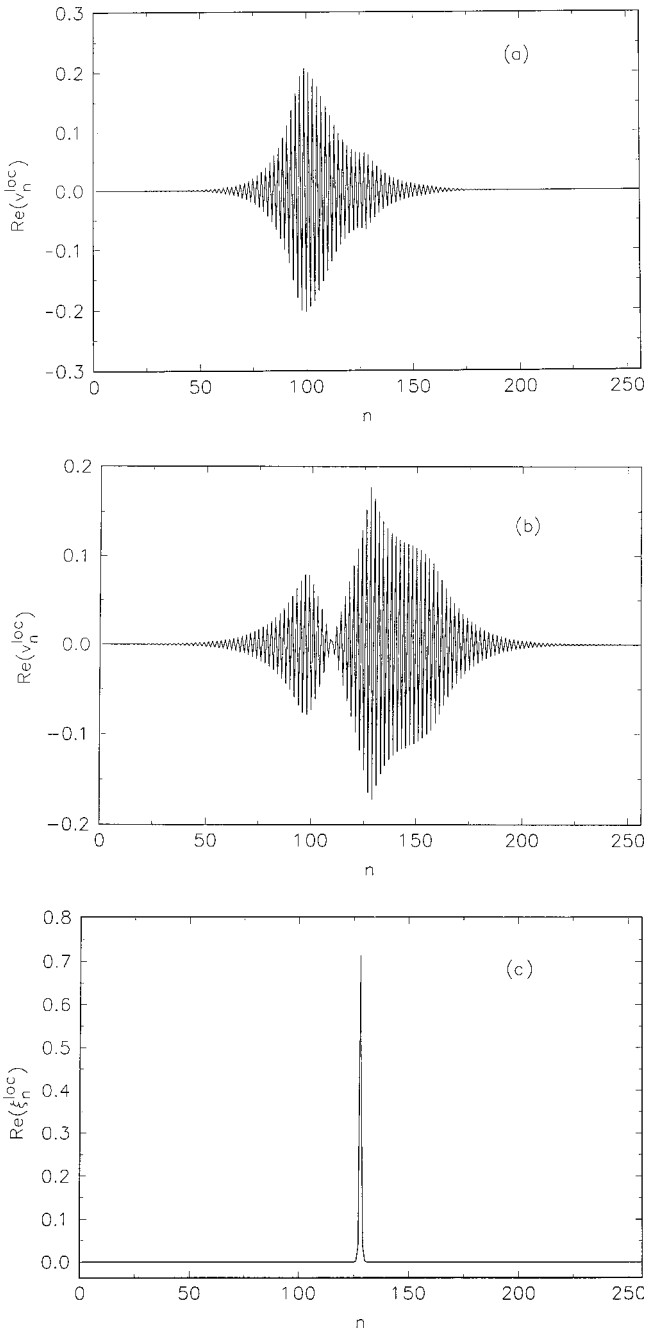

FIG. 5. The real part of the position component v_n^{loc} of the (normalized) eigenvector belonging to the isolated vibronic eigenvalues λ_v^{loc} (a) and $\tilde{\lambda}_v^{loc}$ (b). In (c) the real part of ξ_n^{loc} corresponding to the isolated electronic eigenvalue λ_e^{loc} is shown.

At a later time $(t = 250)$ the isolated electronic eigenvalue λ_e^{loc} has moved upward to the value $1.64i$. The imaginary part of λ_v^{loc} is still detained above the level of the $k = 0$ band edge. Another vibronic eigenvalue $\tilde{\lambda}_v^{loc} = 0.513i$ has left the phonon band, creating a further quasilocalized mode of the KG lattice in addition to the mode shown in Fig. 5(a). In Fig. 5(b) we show the pattern of the real part of the positions

$\tilde{v}_n^{loc}$. There exist two density groups. Compared to the position pattern shown in Fig. 5(a) a further relatively large density group of longer localization length has been created toward the right end of the lattice. The superposition of these two different quasilocalized modes on the KG lattice amplifies the dispersive destruction of the single-site excitation.

These features of the eigenmodes explain (mathematically) the affinity of the vibronic subsystem to distribute energy in its lattice segments where the eigenmodes of Figs. 5(a) and 5(b) have become excited. This temporary energy spreading over the KG lattice is clearly reflected in the evolution of the energetic lattice partition number, which we use to quantify the degree of localization of the partial energies. The energetic lattice partition number is defined as

$$\overline{E}_{e,v}(t)=\left(\frac{\sum_{n=1}^{N} E_{e,v\,n}^2}{\left(\sum_{n=1}^{N} E_{e,v\,n}\right)^2}\right)^{-1}, \tag{17}$$

where $E_{e,v\,n}$ are the local electronic and vibronic energies determined by

$$E_{e\,n}=\frac{\gamma}{2}|c_n|^4+V_0(c_n^* c_{n-1}+c_n c_{n-1}^*), \tag{18}$$

$$E_{v\,n}=\frac{1}{2}p_n^2+\frac{1}{2}\omega_0^2 q_n^2+\frac{1}{4}b q_n^4+\frac{1}{2}c(q_n-q_{n-1})^2. \tag{19}$$

The partial electronic (vibronic) energy is completely confined at a single site if $\overline{E}_{e,v}=1$ and is uniformly extended over the lattice if $\overline{E}_{e,v}$ is of the order N. Thus $\overline{E}_{e,v}$ measures how many sites are excited to contribute to the lattice energy.

With regard to the perturbations of the DNLS breather, we note that the eigenvector corresponding to λ_e^{loc} is now time antisymmetric, i.e., Im $\eta_n^{loc}\neq 0$ and Re $\xi_n^{loc}\neq 0$. However, since the electronic breather and its excited local internal mode still obey the same spatial pattern, the latter is not symmetry breaking with respect to the breather. It is rather that the breather amplitude is modified under radiative losses into the DNLS lattice while the localized shape remains pinned at the originally excited lattice site.

(ii) $300\leqslant t\lesssim 1000$. In this time interval the picture changes significantly. By the sudden steep slope of the energy curves in Fig. 2 we note that the exchange of electronic and vibronic energy becomes much more pronounced. At an instant of time ($t\simeq 310$) the isolated vibron eigenvalue $\tilde{\lambda}_v^{loc}$ has returned to the phonon band whereas λ_v^{loc} has been raised to the value $1.28i$. Now the KG lattice is equipped for the first time with a local breathing mode at the central site, analogous to the one in the $a=0$ case. In this way the vibronic energy starts to accumulate at the initially excited site. The electronic eigenvalue λ_e^{loc} has moved down the imaginary axis to $1.61i$.

From the next snapshot at $t=500$ it becomes apparent that the isolated vibronic eigenvalue $\lambda_v^{loc}=0.52i$ has almost returned to the upper phonon band edge. As a consequence, the local breathing mode ceases to exist and is replaced by a quasilocalized mode. Meanwhile, the electronic isolated eigenvalue has been pushed further downward to a lower imaginary value $1.53i$.

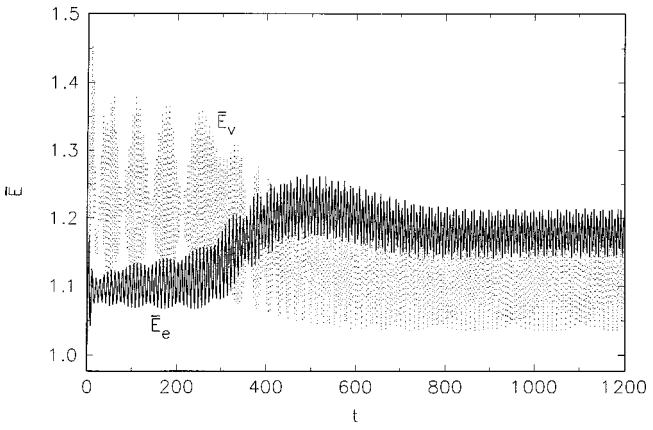

FIG. 6. The lattice partition number defined in Eqs. (17)–(19). Parameters and initial conditions as in Fig. 2 for $a=0.1$.

As time goes by the mobile KG eigenvalue λ_v^{loc} experiences further transitions, that is, it steadily climbs up the imaginary axis. During this process the local breathing KG mode is being rebuilt. At $t=750$ the eigenvalue has reached the point $1.24i$. On its way up the imaginary axis, Im λ_v^{loc} passes the level of Imλ_e^{loc}. The latter is continuing its downward motion and for $t=750$ has dropped down to $1.37i$. We stress that with rising (falling) imaginary part of the eigenvalue the frequency of the corresponding eigenmode gets higher (lower).

During the period of strong exchange interaction between the electronic and vibronic subsystems, there is a temporary increase of the DNLS lattice partition number (see Fig. 6) which is due to radiative losses of the electronic breather amplitude into the DNLS lattice. This emission process can be viewed as a self-stabilization in the sense that in order to maintain its localized shape the electronic breather has to adapt to the reduction of the frequency of its excited internal breathing mode. This is achieved such that the breather diminishes its amplitude and hence its (nonlinear) frequency. To this end the breather has also to get rid of the excess energy that will not be absorbed by the vibron system. In turn, the amount of vibron energy gain is governed by the (growing) excited internal breathing KG mode. Note that neither the DNLS breather nor the KG breather can be made mobile, for there exists no pinning mode in the form of a spatially antisymmetric local internal mode. But the spatially symmetric local breathing mode for the stationary DNLS breather always exists.

(iii) $t\gtrsim 1000$. Finally, all eigenvalues have found their destination on the imaginary axis and the λ spectrum resembles the structure of the uncoupled case (compare Fig. 4), i.e., there are phonon bands and two pairs of isolated purely imaginary conjugate eigenvalues λ_e^{loc} and λ_v^{loc} assigned to the internal local modes of the stable KG and DNLS breathers. However, compared to the $a=0$ case, the isolated eigenvalues have exchanged their positions on the imaginary axis, that is, $\lambda_e^{loc}=1.27i$ and $\lambda_v^{loc}=1.76i$.

Finally, for $t\gtrsim 1000$, when the energy exchange process is over, the DNLS-KG dynamics has approached a stability re-

gime and the electronic and vibronic breathers evolve without further interference. Apart from oscillations around a constant mean value, the nonvarying vibronic and electronic lattice partition numbers assure the strong localization of the partial energies at a few sites of each lattice as seen in Fig. 6.

B. Transition from single- to two-frequency breathers

It is illuminating to describe the different scenarios of the electron-vibron breather interaction also in terms of the power spectrum of the main excitation amplitudes involved. Figure 7(a) depicts the power spectrum of the real part of the central electronic amplitude x_{128} and the vibronic coordinate q_{128}, respectively, measured in the time interval $0 \leqslant t \leqslant 250$. (Note that only the low-frequency part without higher harmonics is shown.) Like the power spectrum of the uncoupled case the present spectrum for the coupled case reveals two peaks at separate incommensurate frequencies where the lower (higher) frequency peak corresponds to the vibronic (electronic) breather motion.

Later, for $t \gtrsim 300$, the pronounced breather interaction process sets in. From spectral analysis performed in the interval $300 < t \leqslant 550$ for either electronic as vibronic amplitude, a second peak emerges between the electronic and vibronic peaks [see Fig. 7(b)]. Their mutual overlap points to resonance interaction between the electronic and vibronic subsystems, viz., their breathers. Consequently, a transition from weakly interacting single-frequency breathers to strongly interacting two-frequency breathers has taken place. As time progresses the height of the left (right) vibronic (electronic) peak of the power spectrum is gradually lowered. Simultaneously, the right (left) vibronic (electronic) peak height is enhanced while the frequency positions move in opposite directions, namely, the electronic peak shifts to lower and lower frequencies and vice versa for the vibronic peak. Eventually, when the breather interaction process has terminated, the power spectrum for $t \gtrsim 1000$ restores two isolated peaks, but the electronic and vibronic peaks have now exchanged their positions compared to the early time power spectrum [see Fig. 7(c)]. This is due to the fact that the electronic breather, after the interaction phase with the vibronic breather, has reduced amplitude and hence also lower frequency. Correspondingly, the vibronic breather has gained amplitude (energy) at the expense of the electronic breather, shifting its power spectrum peak to a higher frequency.

C. Formation of a vibronic phonobreather

We consider the case of stronger coupling between the electron and vibron systems by choosing $a = 0.65$. Again single-site excitations are used. In Figs. 8(a) and 8(b) we draw the spatiotemporal evolution of the DNLS and KG lattices. The narrow excitation peak of the DNLS lattice soon splits into two low-amplitude itinerant breathers. Analysis of the linear stability shows that for the DNLS system an unstable eigenmode with time antisymmetric part has been excited, which causes breather splitting and the subsequent mobility of the remaining two fragments (see also [38]). These breathers are not exact solutions so that their nonuniform movement is restricted to a lattice segment of nearly 40 sites.

On the KG lattice a phonon background is initiated. On top of it a long-lived breather with extended tail (phonobreather [25,52,37]) persists. From the plot of the temporal evolution of the electronic and vibronic energies we deduce that the energy redistribution is in favor of the vibronic system, as seen in Fig. 8(c). The lattice partition number shown in Fig. 8(d) confirms that the vibronic energy remains

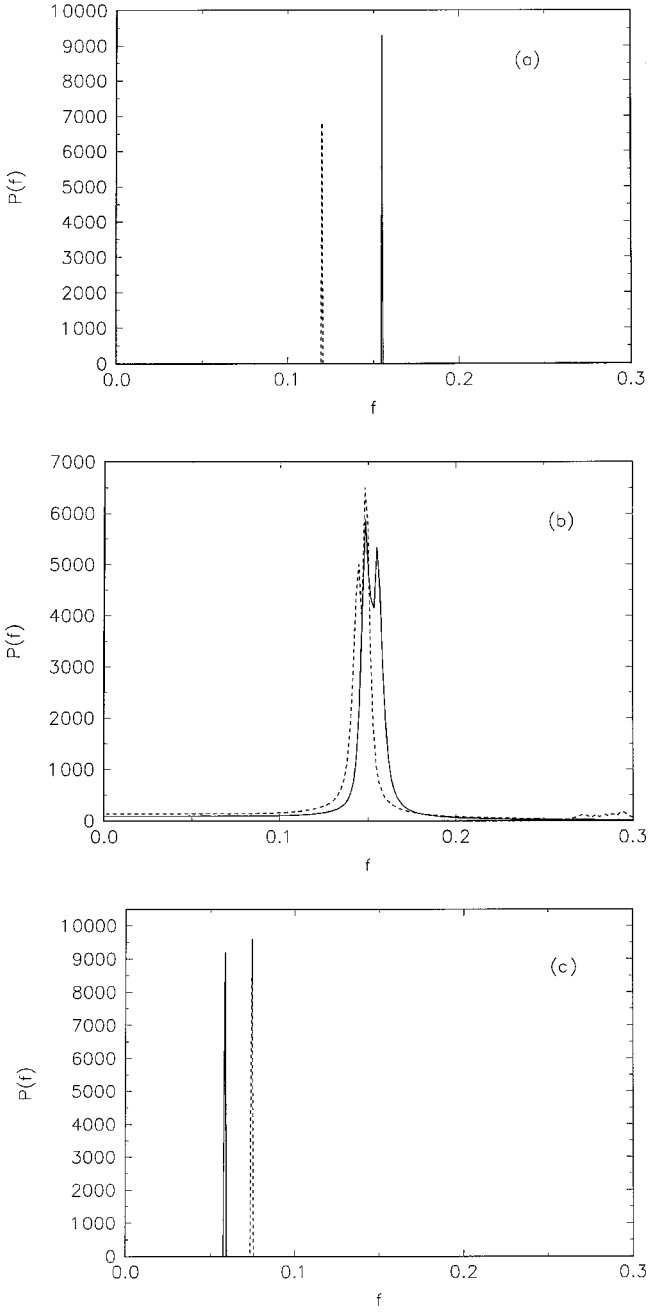

FIG. 7. The temporal development of the power spectrum of the time evolution of the central electronic amplitude x_{128} and the vibronic coordinate q_{128}, respectively; only the low-frequency part without higher harmonics is depicted. (a) The time interval $0 \leqslant t \leqslant 250$. Two isolated peaks at distinct frequencies. The left (right) peak is attributed to a single-frequency KG (DNLS) breather. (b) The time interval $300 < t \leqslant 550$. The KG and DNLS power spectra produce a second peak situated at a frequency between those of (a). Two-frequency breathers are being formed. (c) The time interval $1000 \leqslant t \leqslant 1500$. The reappearance of two isolated peaks at distinct frequencies. The left (right) peak now belongs to the single-frequency DNLS (KG) breather.

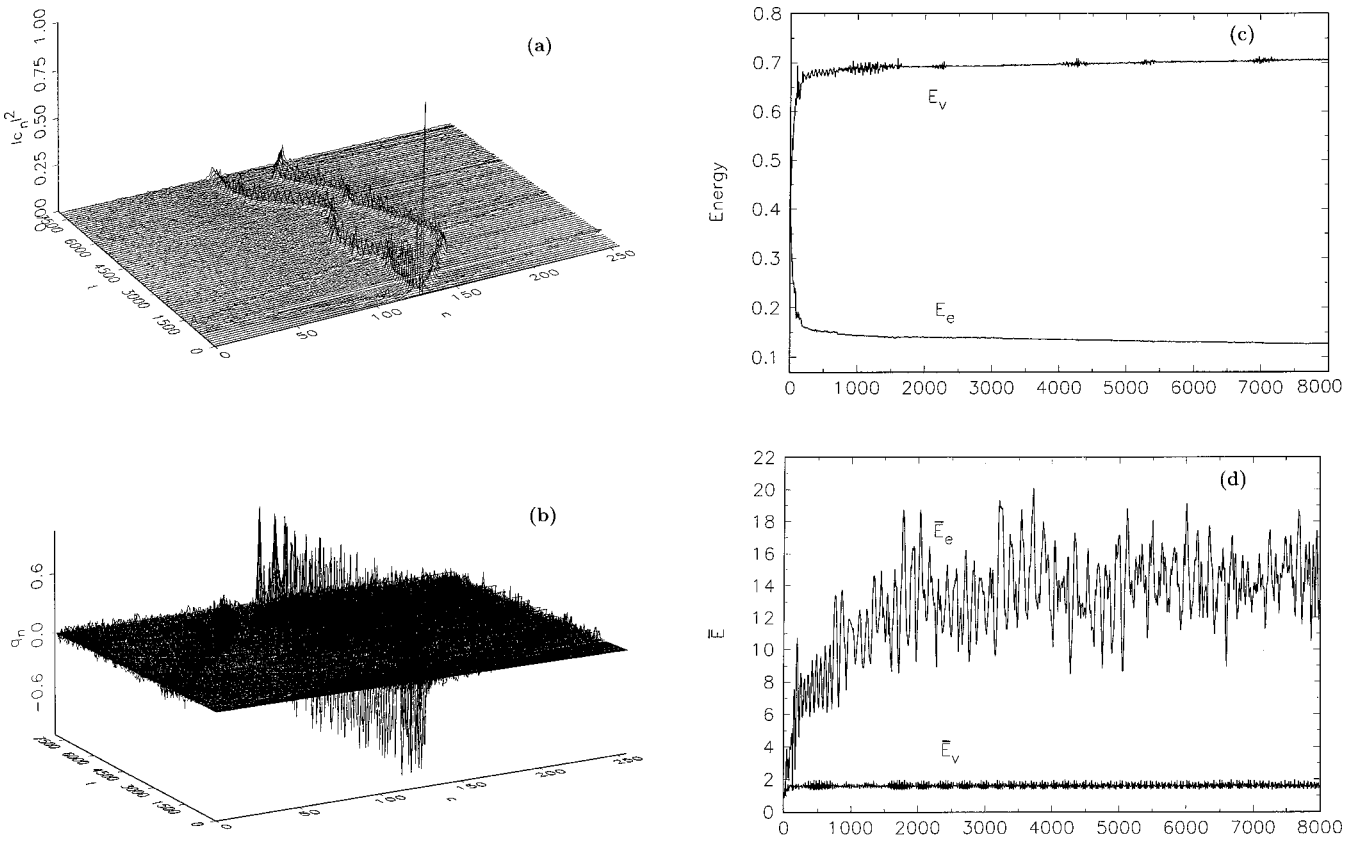

FIG. 8. The coupled DNLS-KG lattice dynamics with single-site excitations according to $x(0)_{128}=y(0)_{128}=1/\sqrt{2}$, $x(0)_{n\neq 128}=y(0)_{n\neq 128}=0$, $q(0)_{128}=1$, $q(0)_{n\neq 128}=0$, and $p(0)_{1\leq n\leq 256}=0$. (a) Spatiotemporal evolution of the electronic occupation number $|c_n(t)|^2$ illustrating the immediate decay of the initial single-site excitation to two low-amplitude itinerant breathers. (b) Spatiotemporal evolution of the vibronic coordinate $q_n(t)$. A phonobreather around the central site has been created. (c) Temporal evolution of the partial energies. The electronic energy E_e drops while the vibronic energy E_v rises. (d) The lattice partition number for the DNLS and KG systems as indicated in the plot. In agreement with the results shown in (a)–(c) the vibronic energy remains localized whereas the electronic energy is spread over the DNLS lattice.

strongly localized whereas the electronic energy is shared by many DNLS lattice sites. The most important consequence of this process physically is that the electron is no longer localized at the initially excited site, unlike in the cases considered in Sec. III. Due to the modulation of the electronic transfer matrix element by numerous extended phonon background modes, electronic transfer into extended parts of the lattice is stimulated. As in Sec. III the vibronic breather of the KG lattice prevents a rapid relaxation.

IV. SUMMARY

We have considered the interaction of electron and vibron breathers in a coupled DNLS-KG lattice system. In the formation process of the breathers a single lattice site has been used electronically and vibrationally. We have always observed temporal energy redistribution in favor of the vibronic degrees of freedom, regardless of the value of the electron-vibron coupling strength. When for weak electron-vibron couplings the energy content of the KG and DNLS system eventually becomes balanced, a stable breather evolves on each lattice. Such a combined electron-vibron bound state has strong influence on the relaxation process subsequent to a local injection of excitation energy in real systems (e.g., solids, biomolecules). Probing the short term relaxation dynamics is of special interest for achieving a steady regime of the coupled electron-vibron lattice system starting from a nonequilibrium state. At short times we observed that the stronger the electron-vibron coupling the more electronic energy is absorbed by the vibronic subsystem to be stored in a vibron breather. During the exchange process the amplitude of the localized electronic state is gradually reduced, but localization of the electron at the initially excited site is maintained. Afterward, when the energy migration is over, the evolution of the electronic and vibrational energies progresses with temporal oscillations decaying faster the larger is the amplitude of the vibron breather. This result demonstrates that in coupled systems excited in nonequilibrium initial states higher-amplitude breathers may significantly boost the relaxation process. The vibron breathers in particular possess an energy absorbing capacity that assists the rapid attainment of an equilibrium regime.

We have discussed the existence and stability of localized internal breathing modes derived from a system of linear equations in tangent space. To this end we have considered the time evolution of the corresponding Lyapunov exponents and the resulting stability properties of the associated eigenfunctions. First we considered the weak coupling case. Remarkably, the DNLS lattice always possesses a local breathing mode assisting permanent energy localization, whereas in the beginning the KG lattice has no such local internal

mode. In the course of time a dynamical process of self-stabilization takes place, during which the KG lattice also produces a stable local internal mode, supporting a breather responsible for the vibron energy localization. Eventually, the lattice dynamics is characterized by two coexisting stable breathers.

Interestingly, above a critical electron-vibron coupling strength, energy localization on only the KG lattice is preferred, where a phonobreather is formed. The electron breather splits up into two small amplitude itinerant breathers that are unable to prevent greater dispersion of the electronic energy.

ACKNOWLEDGMENT

This work was supported by the Deutsche Forschungsgemeinschaft via the Heisenberg-program (He 3049/1-1).

[1] A. J. Sievers and S. Takeno, Phys. Rev. Lett. **61**, 970 (1988).
[2] S. Takeno, J. Phys. Soc. Jpn. **58**, 759 (1989).
[3] J. B. Page, Phys. Rev. B **41**, 7835 (1990).
[4] D. K. Campbell and M. Peyrard, in *Chaos*, edited by D. K Campbell (AIP, New York, 1990), p. 305.
[5] S. Takeno and K. Hori, J. Phys. Soc. Jpn. **60**, 947 (1991).
[6] K. Hori and S. Takeno, J. Phys. Soc. Jpn. **61**, 2186 (1992).
[7] S. Takeno and S. Homma, J. Phys. Soc. Jpn. **60**, 731 (1991), **62**, 835 (1993); S. Takeno, *ibid.* **61**, 2821 (1992); S. R. Bickham, S. A. Kiselev, and A. J. Sievers, Phys. Rev. B **47**, 14 206 (1993); S. R. Bickham, A. J. Sievers, and S. Takeno, *ibid.* **45**, 10 344 (1992).
[8] K. W. Sandudsky, J. B. Page, and K. E. Schmidt, Phys. Rev. B **46**, 6161 (1992).
[9] Ch. Claude, Yu. S. Kivshar, K. H. Spatschek, and O. Kluth, Phys. Rev. B **47**, 14 228 (1992).
[10] T. Dauxois, M. Peyrard, and C. R. Willis, Physica D **57**, 267 (1992); Phys. Rev. E **48**, 4768 (1993); T. Dauxois and M. Peyrard, Phys. Rev. Lett. **70**, 3935 (1993).
[11] Yu. S. Kivshar, Phys. Rev. E **48**, 4132 (1993).
[12] S. Flach and C. R. Willis, Phys. Lett. A **181**, 232 (1993); Phys. Rev. Lett. **72**, 1777 (1994).
[13] S. Flach, C. R. Willis, and E. Olbrich, Phys. Rev. E **49**, 836 (1994).
[14] O. A. Chubykalo, A. S. Kovalev, and O. V. Usatenko, Phys. Lett. A **178**, 129 (1993).
[15] Yu. S. Kivshar and D. K. Campbell, Phys. Rev. E **48**, 3077 (1993).
[16] Yu. S. Kivshar and M. Salerno, Phys. Rev. E **49**, 3543 (1994).
[17] E. W. Laedke, K. H. Spatschek, and S. K. Turitsyn, Phys. Rev. Lett. **73**, 1055 (1994).
[18] S. Aubry, Physica D **86**, 284 (1995).
[19] S. Takeno and M. Peyrard, Physica D **92**, 140 (1996).
[20] G. P. Tsironis and S. Aubry, Phys. Rev. Lett. **77**, 5225 (1996).
[21] A. B. Aceves, C. De Angelis, T. Peschel, R. Muschall, F. Lederer, S. Trillo, and S. Wabnitz, Phys. Rev. E **53**, 1172 (1996).
[22] J. A. Sepulchere and R. S. MacKay, Nonlinearity **10**, 679 (1997).
[23] T. Cretegny and S. Aubry, Phys. Rev. B **55**, 11 929 (1997).
[24] S. Aubry, Physica D **103**, 201 (1996).
[25] S. Flach and C. R. Willis, Phys. Rep. **295**, 181 (1998).
[26] R. S. MacKay and S. Aubry, Nonlinearity **7**, 1623 (1994).
[27] D. Bambusi, Nonlinearity **9**, 433 (1996).
[28] P. Marquié, J. M. Bilbault, and M. Remoissenet, Phys. Rev. E **51**, 6127 (1995).
[29] P. Binder, D. Abraimov, A. V. Ustinov, S. Flach, and Y. Zolotaryuk, Phys. Rev. Lett. **84**, 745 (2000).
[30] H. S. Eisenberg, Y. Silberberg, R. Morandotti, A. R. Boyd, and J. S. Aitchison, Phys. Rev. Lett. **81**, 3383 (1998).
[31] B. I. Swanson, J. A. Brozik, S. P. Love, G. F. Strouse, A. P. Shreve, A. R. Bishop, W.-Z. Wang, and M. I. Salkola, Phys. Rev. Lett. **82**, 3288 (1999).
[32] A. R. Bishop, D. K. Campbell, P. S. Lomdahl, B. Horovitz, and S. R. Phillpot, Phys. Rev. Lett. **52**, 671 (1984); S. R. Phillpot, A. R. Bishop, and B. Horovitz, Phys. Rev. B **40**, 1839 (1989).
[33] A. H. Zewail, Adv. Chem. Phys. **101**, 892 (1997).
[34] T. Rössler and J. B. Page, Phys. Rev. Lett. **78**, 1287 (1998).
[35] D. Chen, S. Aubry, and G. P. Tsironis, Phys. Rev. Lett. **77**, 4776 (1996).
[36] V. M. Burlakov, S. A. Kiselev, and V. N. Pyrkov, Phys. Rev. B **42**, 4921 (1990).
[37] J. L. Marin and S. Aubry, Nonlinearity **9**, 1501 (1996).
[38] M. Johansson and S. Aubry, Nonlinearity **7**, 1151 (1997).
[39] C. Baesens, S. Kim, and R. S. MacKay, Physica D **113**, 242 (1998).
[40] S. Kim, C. Baesens, and R. S. MacKay, Phys. Rev. E **56**, 4955 (1997).
[41] T. Cretegny, S. Aubry, and S. Flach, Physica D **119**, 73 (1998).
[42] D. Bonart, A. P. Mayer, and U. Schröder, Phys. Rev. B **51**, 13 739 (1995); Phys. Rev. Lett. **75**, 870 (1995).
[43] A. Kisilev, S. R. Bickham, and A. J. Sievers, Phys. Rev. B **50**, 9135 (1994).
[44] R. Livi, M. Spicci, and R. S. MacKay, Nonlinearity **10**, 142 (1997).
[45] T. Holstein, Ann. Phys. (N.Y.) **8**, 325 (1959).
[46] A. S. Davydov, J. Theor. Biol. **38**, 559 (1973); A. S. Davydov and N. I. Kislukha, Zh. Éksp. Teor. Fiz. [Sov. Phys. JETP **44**, 571 (1976)]; A. S. Davydov, Phys. Rev. B **25**, 898 (1982).
[47] A. S. Davydov, *Solitons in Molecular Systems* (D. Reidel, Dordrecht, 1985).
[48] E. N. Economou, O. Yanovitskii, and Th. Fraggis, Phys. Rev. B **47**, 740 (1992).
[49] P. L. Christiansen, J. C. Eilbeck, V. Z. Enol'skii, and Yu. B. Gaididei, Phys. Lett. A **166**, 129 (1992).
[50] B. G. Vekhter and M. A. Rather, J. Chem. Phys. **101**, 9710 (1994).
[51] B. G. Vekhter and M. A. Ratner, Phys. Rev. B **51**, 3469 (1995).
[52] S. Aubry, Physica D **103**, 201 (1997).
[53] G. Kalosakas and S. Aubry, Physica D **113**, 228 (1998).
[54] S. Flach and K. Kladko, Phys. Rev. B **53**, 11 531 (1996).
[55] Y. Zolotaryuk and J. C. Eilbeck, J. Phys.: Condens. Matter **10**, 4553 (1998).

[56] J. D. Kress, A. Saxena, A. R. Bishop, and R. L. Martin, Phys. Rev. B **58**, 6161 (1998).
[57] J. C. Eilbeck, P. S. Lomdahl, and A. C. Scott, Physica D **16**, 318 (1985); V. M. Kenkre and D. K. Campbell, Phys. Rev. B **34**, 4595 (1986); A. S. Davydov and N. I. Kuslukha, Phys. Status Solidi B **59**, 465 (1973); D. N. Christodoulides and R. I. Joseph, Opt. Lett. **13**, 794 (1988); N. Finlayson and G. I. Stegeman, Appl. Phys. Lett. **56**, 2276 (1990); Y. Chen, A. W. Snyder, and D. J. Mitchell, Electron. Lett. **26**, 77 (1990); M. I. Molina, W. D. Deering, and G. P. Tsironis, Physica D **66**, 135 (1993); H. Feddersen, P. L. Christiansen, and M. Salerno, Phys. Scr. **43**, 353 (1991); L. J. Bernstein, Opt. Commun. **94**, 406 (1992); D. Hennig, Physica D **64**, 121 (1993); Yu. S. Kivshar, Phys. Rev. E **48**, 4132 (1993); A. B. Aceves, C. De Angelis, T. Peschel, R. Muschall, F. Lederer, S. Trillo, and S. Wabnitz, *ibid.* **53**, 1172 (1996).
[58] R. Scharf and A. R. Bishop, Phys. Rev. A **43**, 6535 (1991).
[59] M. Salerno, Phys. Rev. A **46**, 6856 (1992).
[60] D. Cai, A. R. Bishop, and N. Grønbech Jensen, Phys. Rev. Lett. **72**, 591 (1994).
[61] V. V. Konotop, O. A. Chubykalo, and L. Vázquez, Phys. Rev. E **48**, 563 (1993).
[62] D. Cai, A. R. Bishop, N. Grønbech-Jensen, and M. Salerno, Phys. Rev. Lett. **74**, 1186 (1995); D. Cai, A. R. Bishop, and N. Gønbech Jensen, Phys. Rev. E **52**, 5784 (1995); **53**, 1202 (1996).
[63] D. Hennig, K.Ø. Rasmussen, H. Gabriel, and A. Bülow, Phys. Rev. E **54**, 5788 (1996).
[64] D. Cai, A. R. Bishop, and N. Grønbech Jensen, Phys. Rev. E **53**, 4131 (1996).
[65] P. L. Christiansen, Yu. B. Gaididei, M. Johansson, and K. Ø. Rasmussen, Phys. Rev. B **55**, 5759 (1997).
[66] S. Flach, Physica D **91**, 223 (1996).
[67] M. Michaud, L. Sanche, C. Gaubert, and R. Baudoing, Surf. Sci. **205**, 447 (1988).
[68] L. G. Caron, V. Cobut, G. Vachon, and S. Robillard, Phys. Rev. B **41**, 2693 (1990).
[69] M. Michaud, P. Cloutier, and L. Sanche, Phys. Rev. B **44**, 10 485 (1993).
[70] A. M. Gue, M. Djafari-Rouhani, and D. Esteve, Radiat. Eff. Defects Solids **116**, 219 (1994).
[71] P. F. Bagwell, A. Kumar, and R. Lake, in *Quantum Effect Physics, Electronic and Applications*, edited by K. Ismail, T. Ikoma, and H. I. Smith, IOP Conf. Proc. No. 127 (Institute of Physics, London, 1992).
[72] A. Nakano, R. K. Kalia, and P. Vashista, Appl. Phys. Lett. **62**, 3470 (1993).
[73] M. A. Stroscio, K. W. Kim, G. J. Iafate, M. Dutta, and H. Grubin, Philos. Mag. Lett. **65**, 173 (1992).
[74] D. Kuszner and N. Schwentner, J. Chem. Phys. **98**, 6965 (1993).
[75] N. Schwenter, M. E. Fajardo, and V. A. Apkarian, Chem. Phys. Lett. **154**, 237 (1989).
[76] E. S. Peterson, B. J. Schwartz, and C. B. Harris, J. Chem. Phys. **99**, 1693 (1993).
[77] D. Hennig and G. P. Tsironis, Phys. Rep. **307**, 333 (1999).
[78] C. Kittel *Quantum Theory of Solids* (Wiley, New York, 1987).
[79] D. Hennig (unpublished).
[80] D. Bonart, T. Rössler, and J. B. Page, Physica D **113**, 123 (1998).